IEEE Access
Multidisciplinary | Rapid Review | Open Access Journal

Received July 16, 2019, accepted July 25, 2019, date of publication July 30, 2019, date of current version August 14, 2019.

*Digital Object Identifier 10.1109/ACCESS.2019.2931931*

# Proactive Grooming With Delay Optimization in Sliceable Elastic Optical Network

**WEIQI JIN[1], RENTAO GU[1], YANXIA TAN[1], AND YUEFENG JI[2]**

[1]Beijing Laboratory of Advanced Information Network, Beijing University of Posts and Telecommunications, Beijing 100876, China
[2]State Key Laboratory of Information Photonics and Optical Communications, Beijing University of Posts and Telecommunications, Beijing 100876, China

Corresponding author: Yuefeng Ji (jyf@bupt.edu.cn)

This work was supported in part by the National Key Research and Development Program of China under Grant 2018YFB1800802, and in part by the National Nature Science Foundation of China under Grant 61871051.

**ABSTRACT** Typical energy-efficient dynamic grooming solutions may find a detour and longer path where delay from both the IP layer and optical layer is increased on extra nodes and links. In this paper, analysis of both delay and energy is made on typical grooming operations. An integer linear programming (ILP) model for minimization of both delay and energy is formulized and an alternative model is given with more delay consideration on the distribution over expected IP links. By considering the expected resource distribution of service requests, the available network resource can be re-priced by amortized cost over the expected distribution and a delay proactive control algorithm is designed over this distribution. A proactive delay heuristic is then proposed as an independent policy by a sorting function which is distinguished from other policies by cost functions on a virtual graph. By mining a frequent subset of IP links between node pairs, the problem is simplified without loss of statistical advantage over the resource distribution. The proposed grooming heuristic is performed on a simulation platform in terms of path delay, optical energy consumption, and electrical energy consumption. The simulation results show that the proposed grooming heuristic decreased average path delay without impacting energy performance. Different factors such as sliceability of a network resource, frequent degrees of expected resource, and grooming control periods, which affect the performance of the proposed heuristic, are compared to give thorough evaluations.

**INDEX TERMS** Dynamic traffic grooming, proactive delay control, distribution of IP links, frequent pattern mining, sliceable elastic optical network.

## I. INTRODUCTION

Elastic optical network (EON) has further involved to satisfy the ever spectrally efficient requirement, which is one of the most important technologies for the next generation optical networks [1], [2]. Flexibility of the optical network infrastructure is also evolved in sliceable elastic optical network (SEON) with ever finner spectrum resource [3]–[5]. With bandwidth-variable optical cross-connect (BV-OXC), bandwidth-variable transponder (BVT) and sliceable bandwidth-variable transponder (SBVT), lightpaths can be set up without electrical process at intermediate nodes, which leads to significant cost and energy savings [6]–[8]. As traffic demands have become more diverse and heterogeneous [9], it is impossible to find a uniform granularity that can satisfy all different traffic demands and traffic grooming is indispensable in current network actualities. Traffic grooming improves resource efficiency by aggregating multiple electrical or optical sub-channels onto one optical channel [2], [10]. However, without thorough consideration, grooming solutions within existing lightpaths may provide detour and longer paths to provision flows [11], [12], which increases path delay of accommodated connections. Delay requirements from 5G, data center communications and Industrial Internet of Things [13]–[16] are more stringent in respective networks and demand the infrastructure of optical network [17] to provide low delay for all of them. As delay is attracting more and more attention in service provision and network control, the character to provide both low delay and low energy is greatly needed in dynamic traffic grooming. The problem of proactive control with delay optimization in traffic grooming is to provide routes with less path delay without impacting energy efficiency.

Some previous studies on traffic grooming focus on energy performance by neglecting delay performance or assuming that delay is minimal in SEON. With sliceable

The associate editor coordinating the review of this manuscript and approving it for publication was Zhiguang Feng.

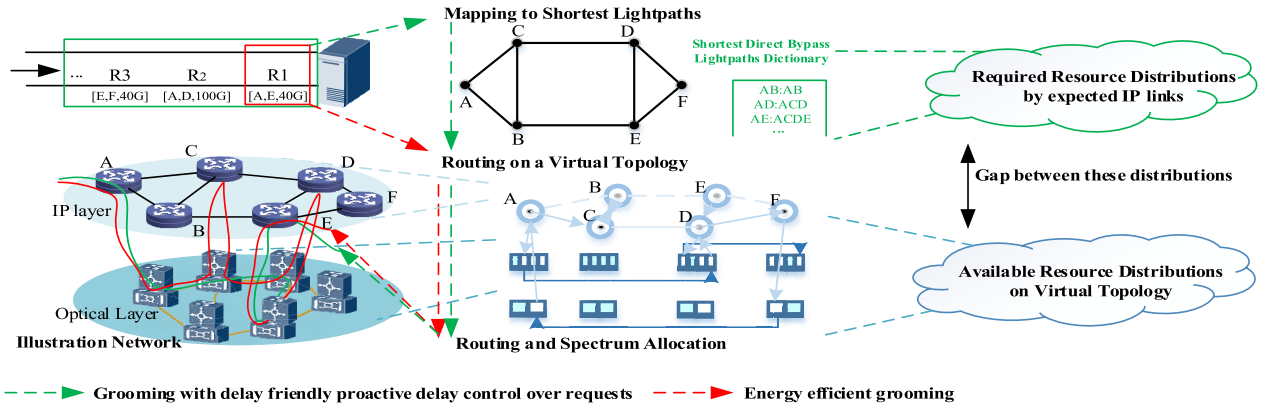


**FIGURE 1.** Grooming over required resource distribution and available distribution.

transponders, traffic grooming becomes more and more effective in decreasing energy consumption and the number of needed router line cards [7]. Traffic requests with suitable demand of bandwidths can be accommodated with less energy consumption produced by amplifiers. Traffic grooming functions can be offloaded from the electrical layer to the optical layer with less optical-electrical-optical (OEO) conversions and less transmission delay. In [10], spectrum reservation schemes and different grooming policies were investigated thoroughly within sliceable-transponder-equipped optical network. An auxiliary graph (AG) [10], [18] is used to estimate network status and to apply grooming policies.

A few studies have investigated delay optimization in IP over wavelength division multiplexing (WDM) networks or EON without considerations of energy or sliceability. The authors in [19] studied delay constrained multicast routing with traffic grooming and formulized the delay constrained grooming problem as an ILP problem. In [20], the proposed algorithm searches an auxiliary graph and sets up dynamic connections based on differential delay constraint and bandwidth allocation granularity. In [21], the authors proposed predictive and incremental (PI) traffic grooming to search with additional predictions. However, useful knowledge in the requests was not represented and utilized to improve network performance. The authors in [11], [12] studied dynamic traffic grooming in IP-over-WDM networks with energy and delay perspectives. Though delay performance is improved, correlations between traffic requests are not fully understood in how path delay is decreased.

Above works lack adequate analysis on service requests, focus only on available resource distributions and search repeatedly without new knowledge learned. Further studies are necessary on the optimization of delay and energy with adequate consideration of request distributions and more sliceability. The sliceability provided by SBVT and other equipments can help improve delay performence with more flexibility to accommodate flows. In typical traffic grooming as in Figure 1, requests are accommodated one by one with a two-step process to avoid NP complexity [22]–[24]. The first step is to find available routes on a virtual topology [10], [18] and the second step is to find available optical resources for these routes. With improved sliceability, there are more choices for both steps to achieve energy efficiency. Delay minimization is more relevent to less detour paths and requires more shortest direct bypass lightpaths (SDBLs) [11], [12]. Improved sliceability can provide convenience for delay and energy control by lowering the cost of building SDBLs. Both energy and delay performance can be improved with increased sliceability and knowledge of request and resource distributions.

However, the increased sliceabilty may also decrease the distribution of existing/available SDBLs and lead to detour paths by grooming operations. It is necessary to study the distributions of SDBLs to achieve low delay and low energy. Delay and energy control by traffic grooming encounters two new problems: 1) For a given set of uncertain traffic requests, what patterns of traffic requests are mostly related to cost of both delay and energy with sliceability improvements? 2) How traffic grooming policies would minimize the cost of both delay and energy with these patterns? These problems can essentially be abstracted to feature design and policy design with learned patterns in a machine learning perspective [27], [28]. Feature design tries to find relations between requests or resources and cost of delay and energy. Policy design helps to lower the cost with adjustable variables or more operations in traffic grooming. Our work in this paper provides solutions to above problems. Works like [11], [12] improve delay performance but fail to reveal critical knowledge related to delay control, which is less instructive and leads to poorer performance than ours.

In this paper, we focus on proactive grooming with delay optimization for SEON. We analyze operations of traffic grooming and formulize the problem in Section II. In Section III, we explore related features, obtain patterns from distributions of both traffic requests and available resources, and design grooming policies to optimize both

delay and energy in SEON. We give numerical results in Section IV and conclusions are presented in Section V.

## II. ANALYSIS AND MODEL FOR DYNAMIC TRAFFIC GROOMING OVER SEON

### A. DELAY AND ENERGY ANALYSIS IN GROOMING OPERATIONS

To accommodate a traffic request, four possible grooming operations may be applied [10]:

- Operation 1: Groom the traffic optically between the source and destination node pairs with/without activating new transmitters and receivers. Establish a new lightpath between node pairs.
- Operation 2: Groom the traffic electrically onto existing lightpaths.
- Operation 3: Split the traffic request; groom some part electrically on existing lightpaths and the other part optically.
- Operation 4: Establish a new lightpath directly for the traffic.

In Operation 4, a new lightpath is established to accommodate a traffic request directly, so delay over the lightpath can be minimized if it is on a SDBL. In Operation 1, 2 and 3, traffic may be groomed over existing lightpaths which may produce longer delay than Operation 4 with more propagation delay on extra links or more transmission delay from extra OEO conversions.

Delay control can be realized by increasing the ratio of Operation 4, i.e., establishing more SDBLs or grooming traffic on SDBLs with Operation 1, 2 and 3. Both require a suitable resource distribution for SDBLs. To prevent over-establishing SDBLs with lower energy efficiency, traffic requests should be analyzed. In [12], traffic requests are sorted in a queue before grooming so requests with higher demand and lower hop distance will be accommodated first. New lightpaths will be established for these prioritized flows first and these lightpaths can be shared with other traffic. More considerations are needed that long flows should be groomed with incident links [25] on shortest paths instead of detour paths.

Energy is consumed by IP ports and optical transponders on source nodes, destination nodes and possible intermediate nodes with OEO conversions. Optical amplifiers also consume energy proportional to the physical length of lightpaths. Because of the energy-traffic proportionality [12], new lightpaths may have less energy efficiency by Operation 4; Operation 1, 2 and 3 are preferred by energy efficient grooming policies.

To decrease energy consumption, various grooming policies are proposed [7] by adjusting the execution order of the four operations. For example, to decrease the OEO conversions, optical grooming is proposed by an execution order of Operation 1-3-2-4. To maximize the ability of electrical grooming, the execution order is changed to Operation 2-3-1-4. Whenever traffic grooming for a connection request is possible, the routing algorithm gives priority to grooming solutions instead of building a SDBL. Delay is assumed to be low in the optical layer and remains unconsidered thoroughly in existing policies in which Operation 4 is applied usually after Operation 1, 2 and 3. However, solutions of operation 4 can also provide less energy consumption by less needed amplifiers if the connections are accommodated on SDBLs.

From above analysis, both delay and energy of a connection are affected by the routes and lightpaths. In this paper, we try to provide proactive delay control by accommodating flows more within the shortest paths, separating existing grooming policies and maintaining energy efficiency.

**TABLE 1. Notations of ILP model for delay and energy control.**

| Notations | Type | Descriptions |
|---|---|---|
| $T^i$ | Set | set of available Transponders of physical node $i$. |
| $C_t$ | Enum | Capacity of transponder $t$. |
| $R^{sd}$ | Set | set of traffic Routes between node pairs $sd$. |
| $R^s, R^d$ | Set | set of traffic Routes with source node $s$ or sink node $d$. |
| $D^{sd}$ | Enum | traffic Demand (Gb/s) of given node pair $sd$. |
| $S^{sd}$ | Enum | Spectrum (GHz) allocated to node pair $sd$. |
| $Sl$ | Integer | number of subtranponders that each transponder can be Sliced. |
| $N^{sd}_{\mathrm{AMP}}$ | Integer | Number of needed AMPlifiers on link $sd$. |
| $G$ | Enum | Guard band between two neighboring flows. |
| $Dl^i_{\mathrm{tran}}$ | Float | Delay of transponder on node $i$. |
| $Dl^{ij}_{\mathrm{path}}$ | Float | path Delay on each traffic of link $ij$. |
| $l_{mn}$ | Set | set of IP links between node $m$ and $n$. |
| $N^{sd}_{\mathrm{AMP}}$ | Integer | number of AMPlifiers used between source node $s$ and destination node $d$. |
| $\alpha$ | Float | relative importance of delay over energy. |

### B. ILP MODEL FOR MINIMIZATION OF DELAY AND ENERGY

In this section, we provide an ILP model of traffic grooming to minimize both delay and energy consumption. We assume that the spectrum resource in the optical network is much larger than needed resource by given traffic loads; the continuous and contiguous spectrum constraints are removed to simplify the model; the processing and transmission delay on nodes are considered in the ILP model but they are much smaller than propagation delay on routes; all the transponders in the network can be sliced to a number of sub-transponders; the delay and power consumption by switch fabric is not considered. For simplicity, we assume a uniform distribution $sd \sim \mathcal{D}_u$ between source-destination node pairs $sd$ in the optical network, traffic demands $D^{sd}$ are bidirectional and satisfy a distribution $D^{sd} \sim \mathcal{D}_d, \mathcal{D}_d = P_1 : P_2 : ... : P_K$, $P_k$ is the proportion of typical bandwidth enumeration, $k \in \{1, 2, ..., K\}$. For example, four types of connection requests: 40, 100, 200 and 400Gbps can be proportional to 5:10:8:2 with $P_1 = 0.2, P_2 = 0.4, P_3 = 0.32, P_4 = 0.08$. Other distributions can also be applied in the following model. The used notations of the ILP model are given in Table 1. Problem statement variables and variables of interest are given below.

*Variables of Problem Statement:*

- $D_{\text{All}}$: Total delay of all connections.
- $P_{\text{IPport}}$: Power consumption of all IP router ports.
- $P_{\text{Otran}}$: Power consumption of all optical transponders.
- $P_{\text{Oamp}}$: Power consumption of all optical amplifiers.
- $P_{\text{PerCard}}$: Power consumption by each IP card.
- $P_{\text{V}}$: Variable part of power consumption by transponders.
- $P_0$: Fix part of power consumption by transponders.
- $P_{\text{A}}$: Power consumption of unit spectrum by amplifiers.

*Variables of Interest:*

- $L_{ij}^{sd}$: equals 1 if lightpath $sd$ uses transmitter $i$ of source node $s$ and reciever $j$ of node $d$.
- $Tr_i^s$: equals 1 if transmitter $i$ of source node $s$ is used.
- $Re_j^d$: equals 1 if reciever $j$ of destination node $d$ is used.

*Objective:*

$$\text{Minimize}(\alpha D_{\text{All}} + P_{\text{IPport}} + P_{\text{Otran}} + P_{\text{Oamp}}) \tag{1}$$

$$D_{\text{All}} = \sum_{sd\in R^{sd}} \sum_{i\in T^s, j\in T^d} (Dl_{\text{path}}^{ij} + Dl_{\text{tran}}^{i} + Dl_{\text{tran}}^{j}) \tag{2}$$

$$P_{\text{IPport}} = P_{\text{PerCard}}(\sum_{s\in R^d} \sum_{i\in T^s} Tr_i^s + \sum_{d\in R^s} \sum_{j\in T^d} Re_j^d) \tag{3}$$

$$P_{\text{Otran}} = \frac{1}{2}(\sum_{s\in R^d} \sum_{i\in T^s} (P_V \sum_{d\in R^s} \sum_{j\in T^d} D^{sd} L_{ij}^{sd} + P_0 Tr_i^s)) + \frac{1}{2}(\sum_{d\in R^s} \sum_{j\in T^d} (P_V \sum_{s\in R^d} \sum_{i\in T^s} D^{sd} L_{ij}^{sd} + P_0 Re_i^d)) \tag{4}$$

$$P_{\text{Oamp}} = \sum_{sd\in R^{sd}} N_{\text{AMP}}^{sd} P_A (S^{sd} + 2G) \tag{5}$$

The ILP model minimizes delay and energy by (1). Sources of delay and energy are given in (2), (3), (4) and (5). The relative importance of delay over energy is given by $\alpha$. Constraints of the problem are given below.

*Constraints:*

$$\sum_{i\in T^s} \sum_{j\in T^d} L_{ij}^{sd} = 1, \quad \forall s, d \tag{6}$$

$$\sum_{d\in R^s} \sum_{j\in T^d} D^{sd} L_{ij}^{sd} \le C_s, \quad \forall s, i \tag{7}$$

$$\sum_{s\in R^d} \sum_{i\in T^s} D^{sd} L_{ij}^{sd} \le C_d, \quad \forall s, j \tag{8}$$

$$\sum_{d\in R^s} \sum_{j\in T^d} L_{ij}^{sd} \le Sl \cdot Tr_i^s, \quad \forall s, i \tag{9}$$

$$\sum_{s\in R^d} \sum_{i\in T^s} L_{ij}^{sd} \le Sl \cdot Re_j^d, \quad \forall s, j \tag{10}$$

Constraint (6) guarantees each pair of source node $s$ and destination node $d$ is connected by any lightpath. Constraint (7) and Constraint (8) ensure the used resource of a transponder does not exceed the capacity of a transponder. Constraint (9) and Constraint (10) ensure that the used sub-transponders do not exceed the maximum number of sub-transponders that each transponder can be sliced.

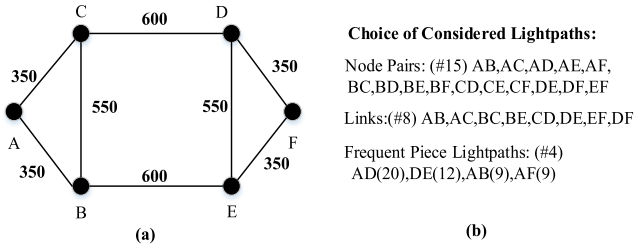


**FIGURE 2.** Exemplary network with six nodes and eight links.

## III. HEURISTIC ALGORITHMS OVER EXPECTED RESOURCE DISTRIBUTIONS

### A. ALTERNATIVE VIEW OF THE CONSIDERED MODEL

The ILP model in prior section decomposes delay and energy onto independent components of SEON. The objective is to minimize delay and energy from components which leads to the decrease of overall delay and energy in the network. Those derived heuristic algorithms from this model can be translated to

$$\text{Minimize } E_{\mathcal{D}_C}[\alpha D_{\text{All}} + P_{\text{IPport}} + P_{\text{Otran}} + P_{\text{Oamp}}], \tag{11}$$

where $\mathcal{D}_C$ is the distribution of network components in SEON, $sd \sim \mathcal{D}_u$ and $D^{sd} \sim \mathcal{D}_d$. The correlations between components are implicitly contained in the constraints. For example, in (2), $Dl_{\text{path}}^{ij}$ is closely related to the IP links (IPLs) between node $i$ and $j$. Different routes produce different delay and energy cost for this link. The route information which affects delay and energy is not given explicitly in the ILP model. Delay is more related to the route selection than energy. Given the route, the delay of a connection on the IP link is fixed while energy cost can be amortized for those variable part as $P_V$ in (4) by grooming more flows on the same IP link. The above ILP model and those derived heuristic algorithms are not delay friendly but energy friendly in this perspective. We propose an alternative delay friendly ILP model over delay and energy by considering resource distribution over IP links.

Additional variables of problem statement:

- $Dl^r$: total delay on route $r$.
- $P^r$: total energy consumption on route $r$.

Objective:

$$\text{Minimize} \sum_{r\in R^{sd}} (\alpha Dl^r + P^r) \tag{12}$$

$$Dl^r = \sum_{l_{mn}\in r} \sum_{i\in T^m, j\in T^n} Dl_{\text{path}}^{mn} + Dl_{\text{tran}}^{m} + Dl_{\text{tran}}^{n} \tag{13}$$

$$\begin{aligned} P^r = \sum_{l_{mn}\in r} \sum_{i\in T^m, j\in T^n} \{ & P_{\text{PerCard}}(Tr_i^m + Tr_j^n) \\ & + \frac{1}{2}(P_V D^{sd} L_{ij}^{mn} + P_0 Tr_i^m) \\ & + \frac{1}{2}(P_V D^{sd} L_{ij}^{mn} + P_0 Re_j^n) \\ & + N_{\text{AMP}}^{mn} P_A (S^{mn} + 2G)\} \end{aligned} \tag{14}$$

*Constraints:* The same as (6)-(10).

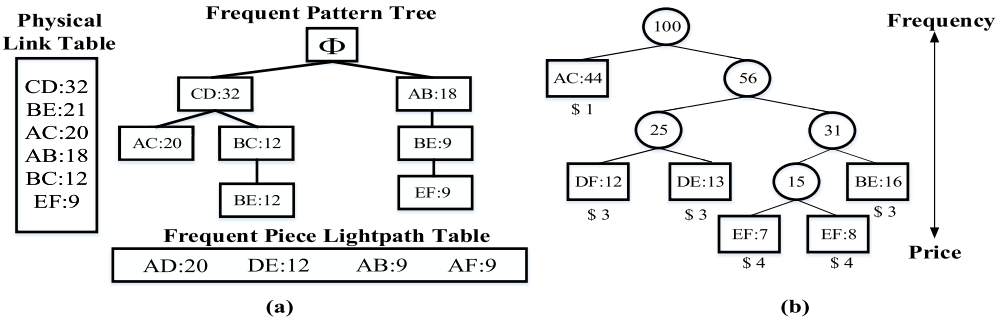


**FIGURE 3.** Frequent pattern tree and cost function for requests of a grooming period.

By integrating delay and energy on IP links in (13) and (14), the delay friendly ILP model maps connections onto IP links which have fixed delay. Both ILP model (1) and (12) are NP-hard but the latter relates to the distributions of the routes. Given the same constraints of (6)-(10), the solution of (12) is also a solution of (1). For a few requests, a distribution on expected routes exists, the problem of proactive control is translated to minimize the objective (12) over this distribution on expected routes. We propose a policy to minimize (12) to groom onto those IP links on SDBLs with least delay and energy by proactive control over the sequence of requests. In the following sections, possible considered IP link sets are analyzed as features of the problem; amortized cost of an IP link is used which is related to frequencies over expected distribution $\mathcal{D}_{\text{IPL}}$; a heuristic algorithm can then be derived to minimize delay and energy on the distribution by

$$\text{Minimize } E_{r\sim\mathcal{D}_{\text{IPL}}}[\alpha D l^r + P^r], \tag{15}$$

with the same traffic distribution $sd \sim \mathcal{D}_u$ and $D^{sd} \sim \mathcal{D}_d$.

### B. DISTRIBUTION OVER IP LINKS

To characterize $\mathcal{D}_{\text{IPL}}$ as features of the problem, we consider possible IP links of both those expected ones by requests and those available ones in SEON as elements of the problem. The node pairs of requests can reveal more useful information by mapping onto shortest paths over physical topology as in Figure 1. We use a 6-node and 8-link butterfly network in Figure 2 (a) as an illustration. Requests are represented as $R(s, d, b)$, where $s$ and $d$ are the source node and destination node; $b$ is the bandwidth demand of the request. The shortest paths of requests [A, E, 4] and [B, F, 4] are A-B-E and B-E-F. They are related by the common link BE on their shortest paths.

To represent the distribution on expected IP links by the requests, we need to define the set of considered IP links in the network. As in Figure 2 (b), one simple solution is to include all IP links on shortest direct bypass routes (SDBRs) of source-destination pairs. The frequencies of IP links on SDBRs need to be estimated and accurate estimation requires lots of requests. Another solution is to include IP links on physical links (PLs) which may lose route information by breaking routes onto separated physical links. The third is to include frequent piece IP links (FPLs), whose frequencies are above a threshold and maintain enough route information. As the cost of delay and energy from network nodes is further reduced, FPLs can be used to groom traffic more efficiently. For example, if AD and DE both are FPLs, AE can be groomed on A-D-E. To efficiently explore those FPLs, we can use FPGrowth [30] algorithm to extract those frequently needed IP links by translating each physical link as a character, as in Figure 3 (a). AD, DE, AB and AF can be selected as FPLs for they are frequently needed by more than 9 requests. Since these FPLs are of high probability to be used and on shortest paths, we only need to consider the amortized cost of requests over distributions of FPLs for (15). Set of IPLs which is out of FPL set is defined as infrequent piece IP link set (IFPL). The cost of FPLs needs to be defined that more frequent FPL is of less cost which guides more traffic onto FPLs.

With FPgrowth algorithm, two important aspectes of knowledge can be obtained. 1) FPLs of expected IP links on those shortest paths can be obtained. With the knowledge on FPLs, traffic grooming can provide a proactive delay control feature by grooming on both SDBLs and FPLs. By setting up lightpaths on these FPLs, grooming solutions can provide shorter physical path with lower path delay and decreased energy consumption by less amplifiers. 2) The frequencies of these FPLs can be estimated. As in Figure 3 (a), the table listed the expected occurrences of each FPL. Another perspective is given in Figure 4 where distributions of requests, desired PLs and FPLs/IFPLs are explicitly given. Mappings of selected requests of AF, BF and BD and marginal distributions are given.

By performing a frequent pattern analysis on service requests and reassigning weights on a virtual graph, delay control can be provided. As in Figure 3 (b), we use Huffman Algorithm to code each IP links with frequencies. IP links with higher occurrences or shorter codes are needed by more requests and should have lower cost that grooming should guide more traffic connections onto these IP links, which is also defined as the control policy.

To represent the available resource distribution in SEON, virtual graphs (VGs) can be used [10], [18]. The cost of

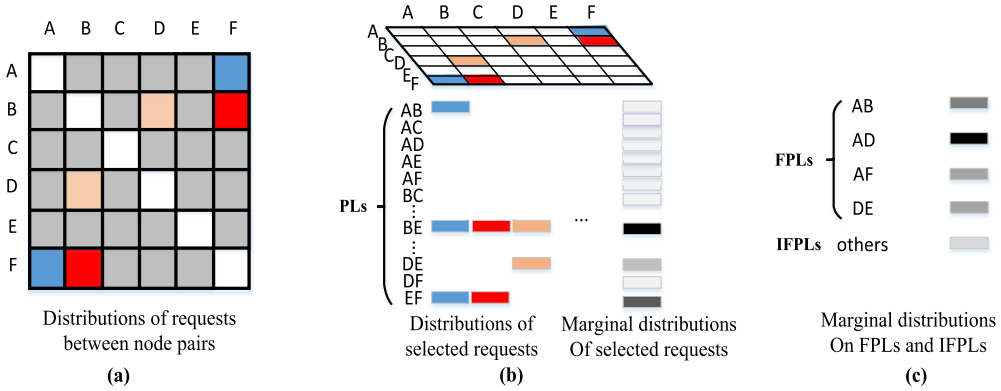


**FIGURE 4.** Distributions over requests on node pairs (a), desired physical links (b) and frequent piece lightpaths/infrequenct frequent piece lightpaths(c).

available IP links should have less cost than that of potential IP links. All available IP links and potential IP links can be represented on a virtual graph by adding edges. Both delay and energy cost of the expected distribution by the requests and the available resource distribution can be integrated on the virtual graph with different cost functions.

**Algorithm 1** Typical Dynamic Traffic Grooming Algorithm

**Input:** Network Status NS, traffic requests $R(s, d, b)$, cost function CF$(*)$ on edges and sorting function SF$(*)$ on requests.

**Output:** Grooming solutions

```
Sort requests in descending order with SF(*) and store them in request queue Q.
Create a virtual graph VG according to NS and assign weights on edges with CF(*).
while Q is not empty do
    Run Dijkstra on VG for Routing (RT).
    if RT succeeds then
        Run Routing and Spectrum Allocation (RSA) in optical layer.
        if RSA succeeds then
            Groom the connection with RT and RSA, pop it from Q, update NS and VG, and reassign weights with CF(*).
        else
            Block the request and pop it from Q.
        end if
    else
        Block the request and pop it from Q.
    end if
end while
```

### C. GROOMING ALGORITHM FOR PROACTIVE DELAY AND ENERGY CONTROL

Typical dynamic traffic grooming algorithm [10] on a virtual graph is described in Algorithm 1. When connection requests $R(s, d, b)$ arrive, they are stored in a request queue and then sorted with a function SF$(*)$. For example, requests can be sorted by the required bandwidth $b$ and requests with larger $b$ will be groomed first. When a request is being accommodated, a virtual graph VG is constructed according to the current network state and edges of VG is assigned with cost function CF$(*)$. After the VG is completely constructed with weights, Dijkstra's algorithm is run to find a route from source node $s$ to destination node $d$. If no route is found on the VG, the request is blocked. If routing (RT) succeeds, then routing and spectrum allocation (RSA) in optical layer will be run for this request. If RSA fail, the connection request will also be blocked. The request will be accommondated with success of both RT and RSA and removed from the request queue.

In our proposed proactive control heuristic, a control period $P_C$ is used for frequent pattern analysis before the request is processed and the FPGrowth algorithm is run on requests in every control period. Those FPLs by traffic requests will be assigned with less weight than weights in typical traffic-grooming policies by CF$(*)$.

To guide more flows onto the FPLs, the cost function CF$(*)$ of edges in the VG need to be redefined. To provide proactive delay control over requests, $\mathrm{cf}_{\mathrm{pdc}}(*)$ is defined on the frequencies of each edge. Each FPL is first coded with Huffman Algorithm and then mapped to discrete cost by the frequency of each edge. The cost for each FPL is set as the length of this code as

$$\mathrm{cf}_{\mathrm{pdc}}(\mathrm{IPL}) = \mathrm{len}(\mathrm{HuffmanCode}(\mathrm{IPL})). \tag{16}$$

The final cost function for each edge $e$ on VG is defined as

$$\mathrm{CF}_{\mathrm{pdc}}(e) = \beta \times \mathrm{cf}_{\mathrm{pdc}}(e) + \mathrm{cf}_O(e), \tag{17}$$

where $\mathrm{cf}_O(*)$ is the cost function of other policies and $\beta$ is the relative importance ratio between proactive delay control and other policies.

### D. DELAY FRIENDLY PROACTIVE CONTROL AS AN INDEPENDENT POLICY

Traffic grooming policies determine how to accommodate a connection with current network resource according to the

intention of the network operator [10]. Current grooming policies focus on energy and transponder savings. By assigning different weights on edges, different traffic grooming policies are achieved. For example, Maximal Electrical Grooming (MEG) and Maximal Optical Grooming (MOG) are proposed to minimize the number of newly established lightpaths on electrical and optical layer. While Minimal number of Virtual Hops (MVH) aims to minimize the number of virtual hops and reduce the number of OEO conversions. Minimal number of Physical Hops (MPH) is proposed to minimize the number of physical hops.

In section B, we have charactered the expected resource distribution $\mathcal{D}_{\text{FPL}}$ and VG is used to character the available existing resource. Both proactive delay control and other grooming policies can be implemented on the same VG by modifying the weights of edges. The total cost of proactive delay control and other grooming policies can be represented as (17). It takes great efforts to determine $\beta$ by understanding IPL distributions of requests and other factors in SEON. To overcome this difficulty, we propose Frequency-First Algorithm (FrFA) as a heuristic algorithm using the distribution of IPLs without determining $\beta$.

Suppose there is a cost threshold $T_C$ below which cost of each request is expected to have. Those requests with less cost are more likely to be below $T_C$ so they should be groomed earlier. To make delay control feature compatible with other policies, the proactive control is performed without modifying the weights on a VG. Instead, the requests are sorted according to the $\text{cf}_{\text{pdc}}$ over the $\mathcal{D}_{\text{FPL}}$ and then RT searches on a VG with the cost function of other policies by setting $\beta = 0$ in (17). The sorting function is redefined as

$$\text{SF}(req) = \sum_{IPL \in \text{SDBR}(req) \cap \text{FPL}} \text{cf}_{\text{pdc}}(\text{IPL}), \tag{18}$$

where *req* is the request being groomed in the request queue. Those requests of lower scores by (18) will be groomed earlier and the cost of used FPLs will be amortized in each grooming period. The communal effect of proactive delay control and other traffic grooming policies will serve together to provide independent performance control.

### E. COMPARISONS WITH OTHER POLICES AND VARIABLES OF INTEREST

Distributions among requests or $\mathcal{D}_{\text{IPL}}$ as a problem feature are more related to delay control which are not fully utilized in Heaviest-first-and-Comparison (HeFC) or Hottest-first and Comparison (HoFC) [11], [12]. In section D, a heuristic algorithm FrFA for proactive delay control is used to retrieve knowledge from distributions over FPLs/IFPLs as $\mathcal{D}_{\text{IPL}}$. By listing the sorting funtion and cost function, comparisons are made in Table 2.

*Theorem 1:* FrFA is the best grooming with least amortized cost on $\mathcal{D}_{\text{FPL}}$.

*Proof:* Let SetIn and SetOut be the set of FPLs and IFPLs. The frequencies over IPLs of SetIn are retrieved and Huffman Code is used. Cost function is defined as the length of the codeword as in Fig. 3 (b). As proved in [29], Huffman Code has least average length with respect to frequencies. Average cost for unit demand of requests will be least by the property of Huffman Code. The cost of connection with bandwidth demand $b$ is lowered by $1b$. FrFA is the best grooming with our policy.

**TABLE 2. Comparisons with other heuristic algorithms.**

| Algorithms | HoFC | HeFC | FrFA |
|---|---|---|---|
| Sorting function | $\frac{b}{\sum \text{cost}(\text{PL})}$ | $\frac{b}{\sum \text{cost}(\text{SDBL})}$ | $\frac{b}{\sum \text{cost}(\text{FPL})}$ |
| Cost function | $\text{cf}_{\text{O}}(e)$ | $\text{cf}_{\text{O}}(e)$ | $\text{cf}_{\text{O}}(e)$ |

*Lemma 2:* The HoFC is one of FrFA with $\mathcal{D}_{\text{IPL}} = \mathcal{D}_{\text{PL}}$ and uniform distribution on $\mathcal{D}_{\text{PL}}$.

*Lemma 3:* The HeFC is one of FrFA with $\mathcal{D}_{\text{IPL}} = \mathcal{D}_{\text{SDBL}}$ and uniform distribution on $\mathcal{D}_{\text{SDBL}}$.

HoFC and HeFC ignore the distribution on $\mathcal{D}_{\text{IPL}}$ which is very important and utilized by FrFA as a problem feature. Then the designed control policy improved delay control by the patterns learned with FPGrowth. The complexity of sorting function in HoFC and HeFC is $O(|R|\log|R|)$. As the number of requests in the queue during a grooming period is small enough, our implementation shows the complexity of the FPGrowth in FrFA is $O(|\text{FPL}|^3)$. All algorithms provides less complexity than that of routing on VT and RSA as $O(|V|^3\log|V|)$.

In [10], sliceability of transponder is considered in power control; energy savings are affected by sliceability of transponders. The more sliceability the transponders are capable of; the more energy savings traffic grooming tends to achieve in a specific scope. In proactive delay control, the available resource distribution on IPLs is also affected by the sliceability. That is because the more sliceability the network have, the less SDBRs may exist in SEON which produce more delay for grooming onto detour routes. Existing IPLs attract more connections than FPLs on SDBRs, proactive delay over the expected distribution may be weaken in some scope of sliceability.

In section C and D, the distribution of IPLs is retrieved within each control period $P_C$. As control period increases, the estimation of the distribution will be more accurate. However, a longer control period also makes later grooming actions less related to $\mathcal{D}_{\text{FPL}}$ estimated earlier. The support threshold $T_S$ of the FPGrowth algorithm also affects the performance of FrFA. The larger the support threshold is, the smaller SetIn is. The estimation on distributions of FPLs will be more focused on most frequent IP links and more distinguishable with those IP links of SetOut.

## IV. NUMERICAL RESULTS

We use a 14-node and 22-link NSF network as in Figure 5 to evaluate the proposed algorithm and follow [10] for most of the implementations of SEON. All the links in the topology are bidirectional links. Node pairs of requests are generated

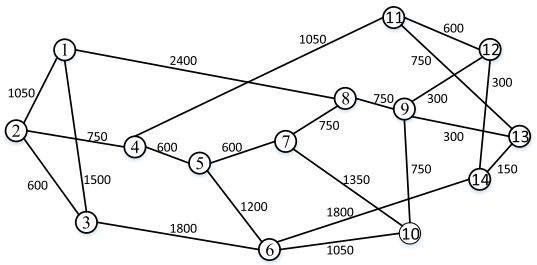


**FIGURE 5.** NSF network with 14 nodes and 22 links.

randomly with a uniform distribution. The arrival and the connection holding time of traffic requests follow a Poisson distribution and a negative exponential distribution with unit mean. There are four types of connection requests: 40, 100, 200 and 400Gbps with the proportion being 6: 10: 3: 1. The granularity of frequency slots (FSs) is 25 GHz and total FSs in each fiber is 300 (7500GHz). The guard band is set as 25GHz. 400Gpbs sliceable optical transponders with 10 subcarriers are used. Each subcarrier can carry a 40 Gbps signal with QPSK modulation. The transponder can also be sliced to 3 sub-transponders that each can carry 4 subcarriers. Each node has 15 transponders. The K-Shortest-Path algorithm with $K = 3$ and First-Fit scheme are used for RSA process. Spectral continuity and contiguity are not restrictions during the grooming process.

The energy consumption model follows [7]. Each Ethernet port consumes 560 W. The power model of transponders is $P_{\text{Otran}}(\text{W}) = 1.683 \times Tr(\text{Gb/s}) + 91.333(\text{W})$. The power model of amplifiers is expressed as $P_{\text{Oamp}}(\text{W}) = 0.0075 \times b(\text{GHz})$ with an extra fixed 30 W by each amplifier. Inline amplifiers are used every 80km. The support threshold $T_S$ of FPGrowth [30] is set as 5. The speed of light in optical fiber is set as $2 \times 10^8$ km/s. The grooming results are averaged over $6 \times 10^5$ requests. The confidence interval is chosen as 90% in the following results.

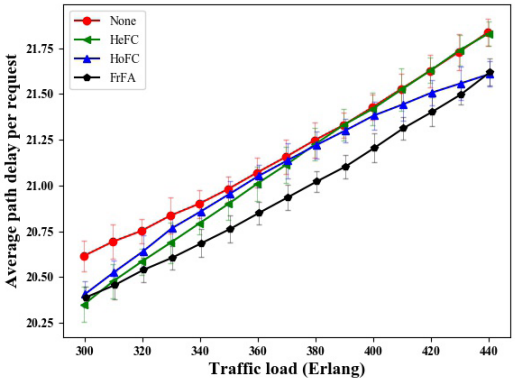


**FIGURE 6.** Average path delay per request with $SI = 4$, $P_C = traffic\ load/2$ and $T_S = 5$.

Figure 6 shows average path delay of all control policies with various traffic loads. HoFC and HeFC succeed in decreasing average path delay by greedily searching paths for less path delay with energy consideration. Average path delay of HoFC is lower than that of HeFC for more detailed expected distribution over PLs by HoFC than the distribution over SDBLs by HeFC when traffic load is above 380 Erlang. As traffic load decreases, HeFC provides less average path than HoFC as SDBLs contain more route information than PLs. FrFA achieves better average path delay performance than both of them in a large range of traffic loads. This is because FrFA explicitly reveals the distribution of the requests over IPLs and searches paths with the knowledge. FrFA uses FPLs/IFPLs which distinguish expected resource distribution by frequencies of IPLs. FPLs/IFPLs in FrFA also contain enough information about routes on SDBLs and ignore information on distribution of IFPLs. As the traffic load increases, average path delay of HoFC decreases faster than that of FrFA and finally becomes comparative. This is because the FPL set or SetIn obtained by FPGrowth approximates PL set of the network. The randomness from request generation and the increasing traffic load also helps connections to be evenly distributed on all FPLs, thus the gain by retrieving the distribution of FPLs decreases. FrFA may achieve better average path delay if the requests have less randomness.

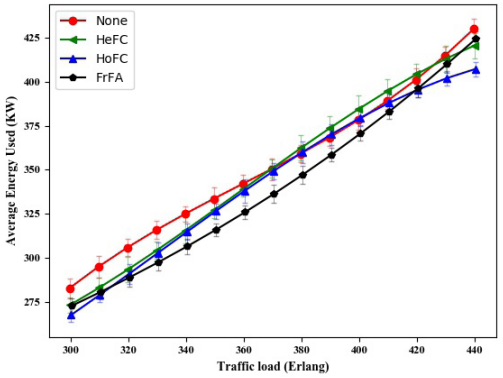


**FIGURE 7.** Average energy consumption with $SI = 4$, $P_C = traffic\ load/2$ and $T_S = 5$.

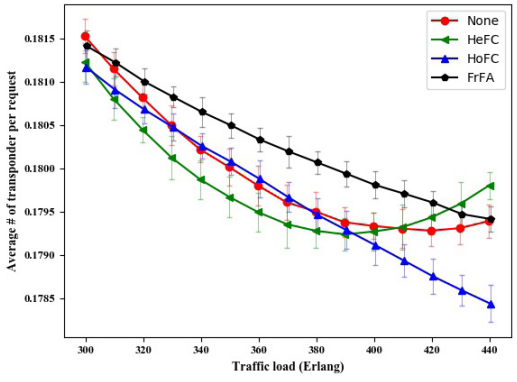


**FIGURE 8.** Average number of used transponders per request with $SI = 4$, $P_C = traffic\ load/2$ and $T_S = 5$.

Figure 7, 8, 9 and 10 show other performances of these policies like average energy consumption, average used

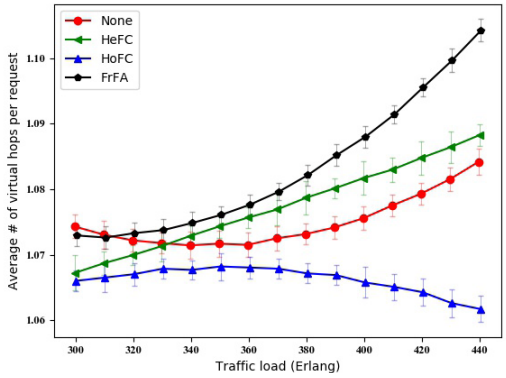


**FIGURE 9.** Average number of virtual hops per request with $Sl = 4$, $P_C$ = *traffic load* /2 and $T_S = 5$.

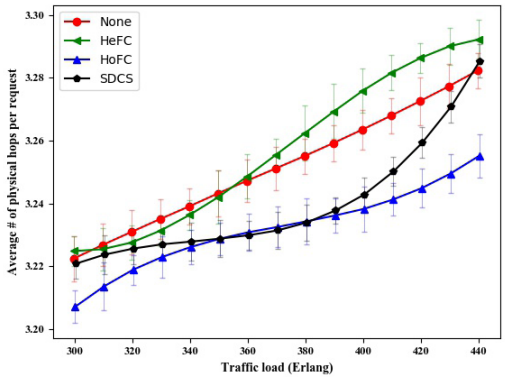


**FIGURE 10.** Average number of physical hops per request with $Sl = 4$, $P_C$ = *traffic load* /2 and $T_S = 5$.

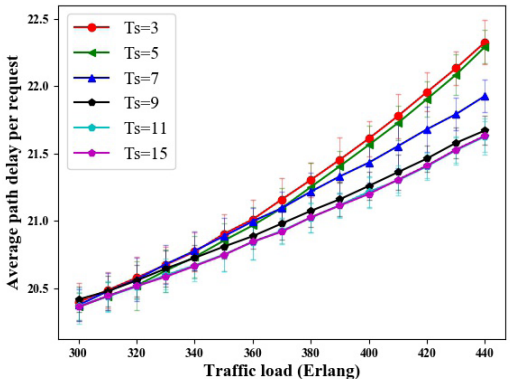


**FIGURE 11.** Delay comparisons among different $T_s$ with $Sl = 4$ and $P_C$ = *traffic load* /2 by FrFA.

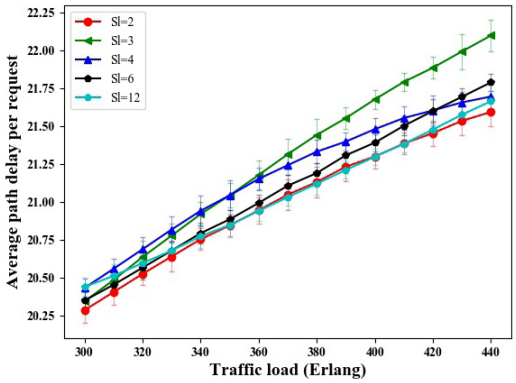


**FIGURE 12.** Delay comparisons among different $Sl$ with $Ts = 5$ and $P_C$ = *traffic load* /2 by FrFA.

transponder, average number of virtual hops and average number of physical hops. In Figure 7, the performance of energy consumption is similar for all policies. FrFA achieves slightly better energy performance than others which comes from less amplifiers on less detour paths. FrFA uses more transponders than others as in Figure 8. This is because FrFA may break an IPL into FPLs and results of virtual hop counts indicate the same effect as in Figure 9. HoFC prefers routes with less physical hops as in Figure 10. By building FPLs more often than other policies, FrFA minimizes average path delay by appropriately increased physical hops with higher frequencies as in Figure 10 which leads to decreased average path delay.

In Figure 11, FrFA is run with different support thresholds. As the support threshold increases from $T_s = 3$ to $T_s = 9$, average path delay of FrFA improves. FrFA distinguishes IPLs between SetIn and SetOut better with increasing $T_s$ and focuses more on IPLs in SetIn. The optimal delay performance is obtained when $T_s = 11$. When $T_s$ goes above 11, the delay performance improves little and begins to decrease slightly. This is because SetIn shrinks as the support threshold increases further. FrFA begins to lose information on expected IPLs with adequate frequency.

In Figure 12, FrFA is run with different sliceability. When $Sl = 2$, the FrFA provides least average path delay. This is because an IPL with larger capacity on DSBLs can provides more available resource for newcomming requests. The distribution of available resource may be much larger than the needed resource distribution by the requests. Lots of requests can be accommodated directly on these DSBLs. As the sliceability of optical network improves, the distribution of these available DSBLs decreases as shown by $Sl = 3, 4, 6$. The optical network begins to provide less available resource distribution on DSBLs. Average path delay is increased by grooming over other IPLs on detour paths. However, as the sliceability further improves, lightpaths are built more by Operation 4 on SDBLs other than grooming or combinations of Operations 1, 2 and 3. Grooming on detour paths is decreased with higher sliceability and average path delay approaches that with $Sl = 2$.

In Figure 13, FrFA is run with different control periods. When $P_C = 180$, FrFA provides least average path delay than other fixed control periods. As the control period increases, average path delay increases first and decreases later. When the control period is small enough, FrFA provides more information on recent requests. When the control period is large enough, FrFA provides detailed information on the distribution over more requests. For those control period beyond above situations, FrFA provides neither recent information nor detailed information which leads to larger

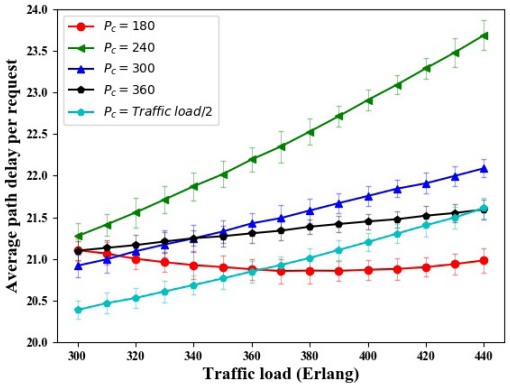


**FIGURE 13.** Delay comparisons among different $P_C$ with $T_s = 5$ and $SI = 4$ by FrFA.

average path delay. The adaptive control period with $P_C = traffic\ load/2$ is shown which lies in the more recent information area and average path delay increases when traffic load increases.

## V. CONCLUSIONS

In this paper, we studied delay and energy cost of grooming operations in SEON. A delay friendly ILP model is formulized to optimize delay and energy on IP links. We characterize the distribution over IP links, reveal the detailed distribution $\mathcal{D}_{\mathrm{FPL}}$ among traffic requests by frequent patterns, and proactively control delay and energy with the distribution. FrFA is proposed as a heuristic to control delay and energy in dynamic traffic grooming with respect to expected resource distribution by traffic requests. The results of numerical experiments indicate that FrFA can be beneficial in terms of delay without impacting energy efficiency. By comparisons with different configurations of FrFA, we give thorough understanding on how the distribution of expected resource helps control delay in dynamic traffic grooming. The increasing flexibility of SEON also exacerbates the complexity and computation of searching possible solutions with performance constraints. The distributions of the traffic requests can be mined to improve network performances. With machine learning concepts, we can abstract more related features and more efficient performance control methods in traffic grooming. The methods we developed in this paper can also be used to other performance control with careful considerations of specific features and control methods. More related and interesting features in the distributions of requests and available resources need to be explored. Both problems are left for our future work.

## REFERENCES

[1] M. Jinno, H. Takara, B. Kozicki, Y. Tsukishima, Y. Sone, and S. Matsuoka, "Spectrum-efficient and scalable elastic optical path network: Architecture, benefits, and enabling technologies," *IEEE Commun. Mag.*, vol. 47, no. 11, pp. 66–73, Nov. 2009.

[2] B. C. Chatterjee, N. Sarma, and E. Oki, "Routing and spectrum allocation in elastic optical networks: A tutorial," *IEEE Commun. Surveys Tuts.*, vol. 17, no. 3, pp. 1776–1800, Aug. 2015.

[3] N. Sambo, A. D'Errico, C. Porzi, V. Vercesi, M. Imran, F. Cugini, A. Bogoni, L. Potì, and P. Castoldi, "Sliceable transponder architecture including multiwavelength source," *IEEE/OSA J. Opt. Commun. Netw.*, vol. 6, no. 7, pp. 590–600, Jul. 2014.

[4] S. Gringeri, B. Basch, V. Shukla, R. Egorov, and T. J. Xia, "Flexible architectures for optical transport nodes and networks," *IEEE Commun. Mag.*, vol. 48, no. 7, pp. 40–50, Jul. 2010.

[5] Y. Wang, X. Cao, Q. Hu, and Y. Pan, "Towards elastic and fine-granular bandwidth allocation in spectrum-sliced optical networks," *J. Opt. Commun. Netw.*, vol. 4, no. 11, pp. 906–917, Nov. 2012.

[6] B. Kozicki, H. Takara, and M. Jinno, "Enabling technologies for adaptive resource allocation in elastic optical path network (SLICE)," in *Proc. Asia Commun. Photon. Conf. Exhib.*, Dec. 2010, pp. 23–24.

[7] J. Zhang, Y. Zhao, X. Yu, J. Zhang, M. Song, Y. Ji, and B. Mukherjee, "Energy-efficient traffic grooming in sliceable-transponder-equipped IP-over-elastic optical networks," *IEEE/OSA J. Opt. Commun. Netw.*, vol. 7, no. 1, pp. A142–A152, Jan. 2015.

[8] M. Hadi and M. R. Pakravan, "Energy-efficient fast configuration of flexible transponders and grooming switches in OFDM-based elastic optical networks," *J. Opt. Commun. Netw.*, vol. 10, no. 2, pp. 90–103, Feb. 2018.

[9] P. S. Khodashenas, J. M. Rivas-Moscoso, B. Shariati, D. M. Marom, D. Klonidis, and I. Tomkos, "Investigation of spectrum granularity for performance optimization of flexible Nyquist-WDM-based optical networks," *J. Lightw. Technol.*, vol. 33, no. 23, pp. 4767–4774, Dec. 1, 2015.

[10] J. Zhang, Y. Ji, M. Song, Y. Zhao, X. Yu, J. Zhang, and B. Mukherjee, "Dynamic traffic grooming in sliceable bandwidth-variable transponder-enabled elastic optical networks," *J. Lightw. Technol.*, vol. 33, no. 1, pp. 183–191, Jan. 1, 2015.

[11] C. Lee and J.-K. K. Rhee "Heated-flow-first traffic grooming for power and delay aware optical network," in *Proc. Int. Conf. Photon. Switching*, Ajaccio, France, Sep. 2012, pp. 1–3.

[12] C. Lee and J.-K. K. Rhee, "Traffic grooming for IP-Over-WDM networks: Energy and delay perspectives," *IEEE/OSA J. Opt. Commun. Netw.*, vol. 6, no. 2, pp. 96–103, Feb. 2014.

[13] H. Yang, J. Zhang, Y. Zhao, Y. Ji, J. Wu, Y. Lin, J. Han, and Y. Lee, "Performance evaluation of multi-stratum resources integrated resilience for software defined inter-data center interconnect," *Opt. Express*, vol. 23, no. 10, pp. 13384–13398, Nov. 2015.

[14] M. Wu, Y. Wu, X. Liu, M. Ma, A. Liu, and M. Zhao, "Learning-based synchronous approach from forwarding nodes to reduce the delay for industrial Internet of Things," *EURASIP J. Wireless Commun. Netw.*, vol. 2018, no. 1, p. 10, Dec. 2018.

[15] C. X. Mavromoustakis, G. Kormentzas, G. Mastorakis, A. Bourdena, E. Pallis, and C. D. Dimitriou, "Joint energy and delay-aware scheme for 5G mobile cognitive radio networks," in *Proc. IEEE Global Commun. Conf.*, Dec. 2014, pp. 2624–2630.

[16] Y. Ji, J. Zhang, X. Wang, and H. Yu, "Towards converged, collaborative and co-automatic (3C) optical networks," *Sci. China Inf. Sci.*, vol. 61, no. 12, Nov. 2018, Art. no. 121301.

[17] Y. Ji, J. Zhang, Y. Xiao, and Z. Liu, "5G flexible optical transport networks with large-capacity, low-latency and high-efficiency," *China Commun.*, vol. 16, no. 5, pp. 19–32, May 2019.

[18] Y. Zhao, R. Tian, X. Yu, J. Zhang, and J. Zhang, "An auxiliary graph based dynamic traffic grooming algorithm in spatial division multiplexing enabled elastic optical networks with multi-core fibers," *Opt. Fiber Technol.*, vol. 34, pp. 52–58, Mar. 2017.

[19] H.-H. Yen, S. S. W. Lee, and B. Mukherjee, "Traffic grooming and delay constrained multicast routing in IP over WDM networks," in *Proc. IEEE Int. Conf. Commun.*, Beijing, China, May 2008, pp. 5246–5251.

[20] W. Lu, X. Zhou, L. Gong, M. Zhang, and Z. Zhu, "Dynamic multi-path service provisioning under differential delay constraint in elastic optical networks," *IEEE Commun. Lett.*, vol. 17, no. 1, pp. 158–161, Jan. 2013.

[21] Z. Ye, X. Cao, X. Gao, and C. Qiao, "A predictive and incremental grooming scheme for time-varying traffic in WDM networks," in *Proc. IEEE INFOCOM*, Turin, Italy, Apr. 2013, pp. 395–399.

[22] K. Christodoulopoulos, I. Tomkos, and E. A. Varvarigos, "Elastic bandwidth allocation in flexible OFDM-based optical networks," *J. Lightw. Technol.*, vol. 29, no. 9, pp. 1354–1366, May 1, 2011.

[23] S. Shirazipourazad, C. Zhou, Z. Derakhshandeh, and A. Sen, "On routing and spectrum allocation in spectrum-sliced optical networks," in *Proc. INFOCOM*, Apr. 2013, pp. 385–389.

[24] H. Wu, F. Zhou, Z. Zhu, and Y. Chen, "Analysis framework of RSA algorithms in elastic optical rings," *J. Lightw. Technol.*, vol. 37, no. 4, pp. 1113–1122, Feb. 15, 2018.

[25] A. Mathew, T. Das, P. Gokhale, and A. Gumaste, "Multi-layer high-speed network design in mobile backhaul using robust optimization," *IEEE/OSA J. Opt. Commun. Netw.*, vol. 7, no. 4, pp. 352–367, Apr. 2015.
[26] G. Shen and R. S. Tucker, "Energy-minimized design for IP over WDM networks," *IEEE/OSA J. Opt. Commun. Netw.*, vol. 1, no. 1, pp. 176–186, Jun. 2009.
[27] F. N. Khan, Q. Fan, C. Lu, and A. P. T. Lau, "An optical communication's perspective on machine learning and its applications," *J. Lightw. Technol.*, vol. 37, no. 2, pp. 493–516, Jan. 15, 2019.
[28] J. Mata, I. de Miguel, R. J. Durán, N. Merayo, S. K. Singh, A. Jukan, and M. Chamania, "Artificial intelligence (AI) methods in optical networks: A comprehensive survey," *Opt. Switching Netw.*, vol. 28, pp. 43–57, Apr. 2018.
[29] T. H. Cormen, C. E. Leiserson, R. L. Rivest, and C. Stein, *Introduction to Algorithms*, 3rd ed. London, U.K.: MIT Press, 2009.
[30] J. Han, J. Pei, Y. Yin, and R. Mao, "Mining frequent patterns without candidate generation: A frequent-pattern tree approach," *Data Mining Knowl. Discovery*, vol. 8, no. 1, pp. 53–87, 2004.

**WEIQI JIN** received the B.S. degree from the Chongqing University of Posts and Telecommunications (CQUPT), in 2012. He is currently pursuing the doctoral degree with the State Key Laboratory of Information Photonics and Optical Communications, Beijing University of Posts and Telecommunications (BUPT). His research interests include machine learning, flexible optical network, and IP-optical integration network design and optimization.

**RENTAO GU** received the B.E. and Ph.D. degrees from BUPT, Beijing, China, in 2005 and 2010, respectively. From 2008 to 2009, he was a Visiting Scholar with the Georgia Institute of Technology, Georgia, USA. He is currently a Professor with the School of Information and Telecommunication Engineering, BUPT. His current research interests include access network and intelligent information processing.

**YANXIA TAN** received the B.S. degree from the Chongqing University of Posts and Telecommunications (CQUPT), in 2013. She is currently pursuing the doctoral degree with the State Key Laboratory of Information Photonics and Optical Communications, Beijing University of Posts and Telecommunications (BUPT). Her research interests include flexible optical network and IP-optical integration network design and optimization.

**YUEFENG JI** received the Ph.D. degree from BUPT, Beijing, China, where he is currently a Professor. His research interests include in the areas of broadband communication networks and optical communications, with emphasis on key theory, and realization of technology and applications.